

Endocytosis of Nanoparticles

Karandeep Singh

*A dissertation submitted for the partial fulfilment
of BS-MS dual degree in Science*



Indian Institute of Science Education and Research Mohali
April 2014

Certificate of Examination

This is to certify that the dissertation titled **Endocytosis of Nanoparticles** submitted by **Karandeep Singh** (Reg. No. MS09071) for the partial fulfillment of BS-MS dual degree programme of the Institute, has been examined by the thesis committee duly appointed by the Institute. The committee finds the work done by the candidate satisfactory and recommends that the report be accepted.

Dr. Dipanjan Chakraborty

Dr. Rajeev Kapri

Dr. Abhishek Chaudhuri
(Supervisor)

Dated: April 24, 2014

Declaration

The work presented in this dissertation has been carried out by me under the guidance of Dr. Abhishek Chaudhuri at the Indian Institute of Science Education and Research Mohali.

This work has not been submitted in part or in full for a degree, a diploma, or a fellowship to any other university or institute. Whenever contributions of others are involved, every effort is made to indicate this clearly, with due acknowledgement of collaborative research and discussions. This thesis is a bonafide record of original work done by me and all sources listed within have been detailed in the bibliography.

Karandeep Singh
(Candidate)

Dated: April 24, 2014

In my capacity as the supervisor of the candidate's project work, I certify that the above statements by the candidate are true to the best of my knowledge.

Dr. Abhishek Chaudhuri
(Supervisor)

Acknowledgements

I would like to thank a number of people whose guidance, support and friendship have not only made this work possible, but also enjoyable. At the very outset I would like to thank my advisor, Dr. Abhishek Chaudhuri for providing me with the opportunity to work in his group, for his encouragement and constant support. He taught me the techniques that will hopefully guide me through a life of good science. I would like to thank all my friends, who were always there for me whenever I needed them and also made my life enjoyable at our Institute. Last but not the least, I thank God for blessing me with a wonderful family, my parents and sisters, without whose support all this would not have been possible.

List of Figures

1.1	Cartoon representation of a cell (<i>Reproduced from Pearson Benjamin Cummings</i>).	1
1.2	Pathways of endocytosis (<i>Reproduced from Canton and Battaglia [2]</i>) . . .	3
1.3	Snapshots of a cross section through a rigid nanoparticle translocating across a planar lipid bilayer membrane immersed in solvent. (<i>Reproduced from Shillcock [28]</i>).	5
1.4	A cross section through a membrane invagination driven by the presence of rigid inclusions (<i>Reproduced from Deserno ([32])</i>)	6
2.1	Figure representing the geometry of the wrapping process. A spherical particle of radius a wraps to the membrane with a degree of wrapping given by $z = 1 - \cos \alpha$. Cylindrical geometry is assumed.	8
2.2	Energy \tilde{E} as a function of the penetration z for rescaled tension $\tilde{\sigma} = 1$ when $E_{\text{free}} = 0$ for different \tilde{w} . $\tilde{w} = 3$ (red), $\tilde{w} = 4$ (green), $\tilde{w} = 5$ (blue) and $\tilde{w} = 6$ (pink).	10
2.3	Energy \tilde{E} as a function of the penetration z for rescaled tension $\tilde{\sigma} = 1$ when $E_{\text{free}} \neq 0$ for different \tilde{w} . $\tilde{w} = 3$ (red), $\tilde{w} = 4$ (green), $\tilde{w} = 5$ (blue) and $\tilde{w} = 6$ (pink).	13
3.1	Model of the system.	16
3.2	Snapshot of the system.	17
3.3	$\frac{c_i(t \rightarrow \infty)}{c_{ex}^0}$ as a function of time.	19
3.4	Normalized particle uptake versus time for different endocytosis rates of the cargo.	21
3.5	Normalized cellular uptake for different endocytosis rates for different ratios of k_{ic}/k_{oc}	22
3.6	Normalized particle uptake for different k_{ic}/k_{oc} rates.	22

3.7	Phase diagram indicating regions for optimal transport. Color bar is the time axis.	23
3.8	Size dependent cellular uptake of non-interacting NP's.	24
3.9	Size dependent variation of endocytosis rate.	24

Abstract

Endocytosis is a highly complex mechanism which the cell uses not only to take up nutrients but also in cell-cell communication. After the endocytosis process is complete, the internalized cargo undergoes a series of dynamics processes like fission, fusion and degradation, which defines the endocytic pathway. In this work, our aim is to analyze some of these processes from a physicist's point of view. In the first part of our work, we focus on a specific type of endocytosis which is called receptor mediated endocytosis. In this process, the cargo which is to be endocytosed is coated with ligands and these ligands bind to specific receptors on the cell membrane. This binding releases chemical energy which is required to overcome the cost of bending the elastic membrane. It is possible to write down a free energy for this process and show the importance of the size of the cargo in the endocytosis process. We are trying to understand the role of interactions, either via the cell membrane or direct interactions between cargo particles, in the endocytosis process.

In the second part of our work, we consider several such cargo as they are internalized and their subsequent dynamics. Here, we do simulation of these cargo particles. In our model we have rates of the different events like endocytosis, exocytosis, fission, fusion, degradation etc. We do Brownian dynamics and our particles are point particles. All the different events that we mentioned about are included as reactions with specific rates. Here our goal is to understand the importance of each of these rates in the trafficking process as well as the distribution of cargo in the endosomal compartments.

Contents

List of Figures	vi
Abstract	vii
1 Introduction	1
1.1 The cell	1
1.2 What is endocytosis ?	2
1.3 Endocytosis and the cell membrane	2
1.3.1 Cell membrane	2
1.4 Understanding cellular uptake of nanoparticles : Simulations	4
1.4.1 Mesoscopic simulation of membranes	5
1.5 Simulating the entire endocytic pathway	6
2 Single particle endocytosis	7
2.1 Various energy contributions	7
2.2 Considering all the energy terms	11
2.2.1 Full energy term and shape equations	11
2.2.2 Necessary boundary conditions	12
3 Multiscale modeling of nanoparticle transport across the cell membrane	15
3.1 Endocytic Transport	16
3.2 Modeling transport of nanoparticles carrying cargo	19
3.2.1 Size dependent cellular uptake	23
3.3 Conclusions	24

Chapter 1

Introduction

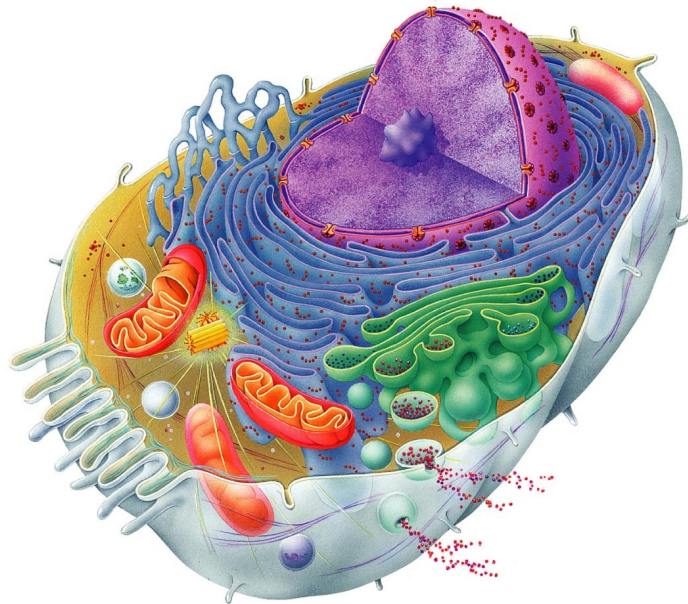


Figure 1.1: Cartoon representation of a cell (*Reproduced from Pearson Benjamin Cummings*).

1.1 The cell

The cell is the basic building block of life [1]. Life is reliant on the consumption and dissipation of energy and these are processes that are occurring all the time inside the cell. A cell is defined by the cell membrane which separates the internal environment of the cell

from the external, the cytoplasm which is the liquid internal environment of the cell, and the numerous functional and structural entities like the cytoskeleton and the cellular organelles which exist within this liquid environment. The membrane, cytoskeleton and the extracellular matrix together provides the structural integrity of the cell.

1.2 What is endocytosis ?

Endocytosis is one of the most important processes that is used by cells to internalize molecules and macromolecules. However, its importance is not limited to only the uptake of nutrients because endocytosis is required for performing a large number of other functions such as cell adhesion and migration and the signalling of cell surface receptors. What is an important mechanism for the cell to sustain the various life processes can be its demise - the endocytic process is also used by bacteria and viruses to invade cells ! Understanding the mechanisms that regulate endocytosis is also extremely vital in the cellular uptake of nanoparticles which are routinely used in targeted drug delivery. This is also the main focus of this project work.

The endocytic process can be separated into the following basic mechanisms :

- selection and segregation of the cargo at the cell surface
- subsequent invagination and pinching off from the cell membrane
- transport of these membrane wrapped cargo, called vesicles, to compartments within the cells where they fuse with the target membrane thus releasing the cargo.

The mechanisms by which specific cargo are internalized differ in their morphological and biochemical details. (Fig.1.2)

1.3 Endocytosis and the cell membrane

As we have discussed in detail the cell membrane plays a key role in the endocytic mechanism. Here, we briefly talk about the cell membrane.

1.3.1 Cell membrane

The cell membrane is a lipid bilayer membrane behaving as a fluid in physiological temperatures. The lipids can diffuse freely within each leaflet of the bilayer. The fluidity of

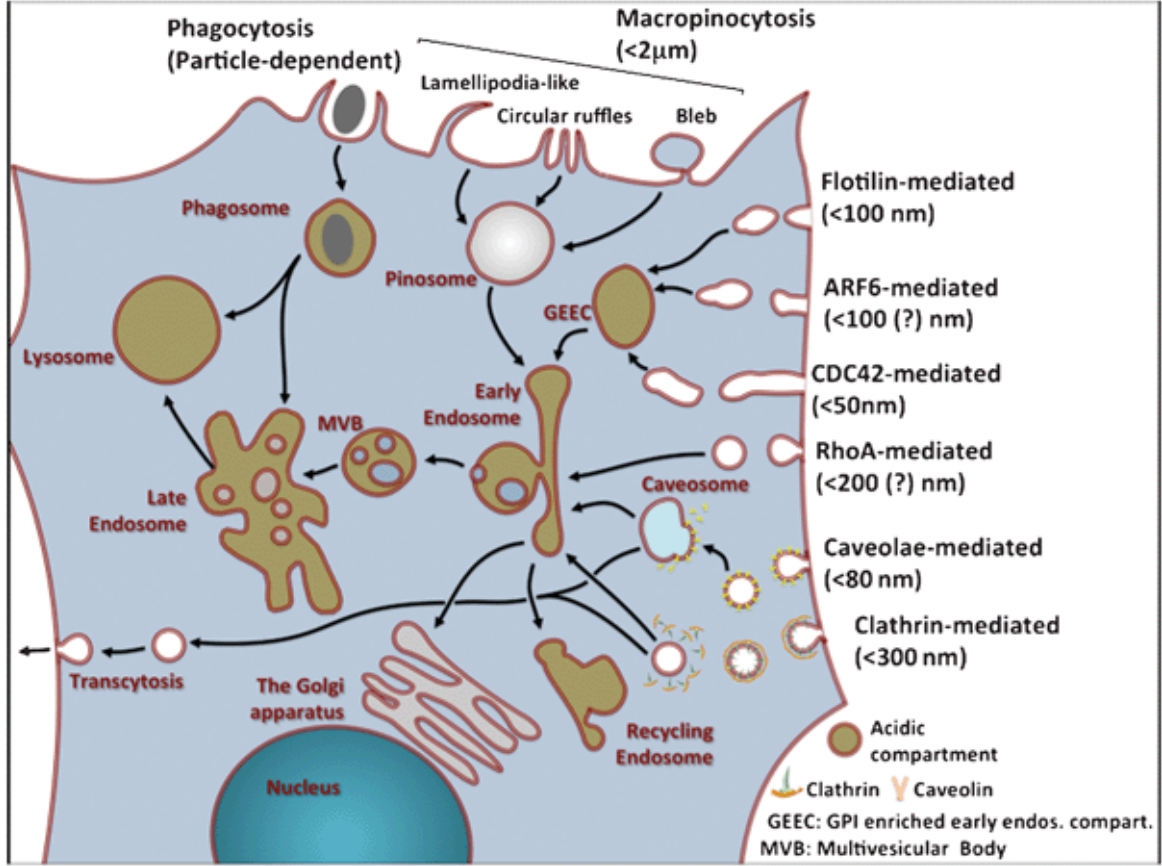


Figure 1.2: Pathways of endocytosis (*Reproduced from Canton and Battaglia [2]*)

the membrane implies that it cannot resist shear stresses. Therefore there is no deformation energy cost in shearing the membrane. The lipid bilayer is often modeled as a two-dimensional surface embedded in three-dimensional space. The energy associated with the surface is described by a Hamiltonian which depends on the surface geometry. It costs energy to bend the membrane and this energy cost is given by quadratic expressions of the curvature. Now at each point on the surface one can define two principal curvatures, k_1 and k_2 . It is more convenient to work with the mean curvature, $k_1 + k_2$, and the gaussian curvature $k_1 k_2$ rather than individual principal curvatures. Including surface tension, the complete Hamiltonian is then according to Helfrich [3, 4] :

$$\mathcal{H} = \int dA \left[\sigma + \frac{\kappa}{2} (k_1 + k_2 - c_0)^2 + \bar{\kappa} k_1 k_2 \right] \quad (1.1)$$

where the integral extends over the entire membrane surface and dA represents the intrinsic area element. The parameters σ , κ , c_0 and $\bar{\kappa}$ are the surface tension, bending rigidity,

spontaneous curvature and the gaussian curvature modulus respectively. A number of experimental and theoretical studies [5, 6, 7, 8] have shown that the energy associated with the membrane is dominated by bending. Therefore for all practical purposes we may set $\sigma = 0$. Also for symmetric membranes (identical on both sides) $c_0 = 0$.

The *curvature model* has been used extensively to study a host of physical phenomena involving membranes : vesicle shapes [8, 9, 10, 11, 12, 13], vesicle adhesion [14, 15], colloidal wrapping [16, 17] or tether pulling [18, 19, 20, 21, 22]. For example, in aqueous solution bilayers typically form closed surfaces or vesicles. It is energetically favorable to do so. The shape of a vesicle with surface area A and volume V is determined by minimizing $\mathcal{H} + PV + \Sigma A$ where P denoted the pressure difference between the two sides and Σ denotes the lateral tension. In thermal equilibrium vesicles attain the shape that corresponds to the minimum bending energy and the curvature model is successful in explaining these minimal shapes. Recently, Liu et. al. [23] have developed a mechanochemical model to explain the temporal and spatial progression of endocytic events leading to vesicle scission. In their model the central idea is that the membrane curvature is coupled to the accompanying biochemical reactions.

1.4 Understanding cellular uptake of nanoparticles : Simulations

Computer simulation provides an important tool to understand the cellular processes and to computationally test hypotheses about such processes in a quantitative manner. To understand the endocytosis of nanoparticles (NP), the first step would be to model the cell membrane. There are a number of excellent reviews [24, 25, 26, 27, 28] that discuss the simulation techniques that have been developed for the study of biological membranes. However if one is interested in understanding the endocytic pathway in full detail, then explicit modeling of cell membrane is difficult and we may choose to perform rate dependent stochastic simulations. We first give a brief outline of studies on simulation of membranes and of nanoparticle uptake. We then discuss a possible model for the endocytic pathway.

1.4.1 Mesoscopic simulation of membranes

An all atom molecular dynamics (MD) simulation [29] is the most accurate simulation method. However this is computationally prohibitive more so when we would like to investigate membrane dynamics where lengths scales of the order of tens of nanometers have to be studied over a few microseconds of time where groups of atoms are replaced by particles or *beads*, so one does coarse grained simulations. The cell membrane is a lipid bilayer membrane. Lipids are amphiphiles and they spontaneously self assemble into complex structures such as two-dimensional membranes. Any coarse grained simulation would have to keep these basic properties intact. There are indeed quite a number of coarse grained methods that do so and we discuss a few of the more relevant ones.

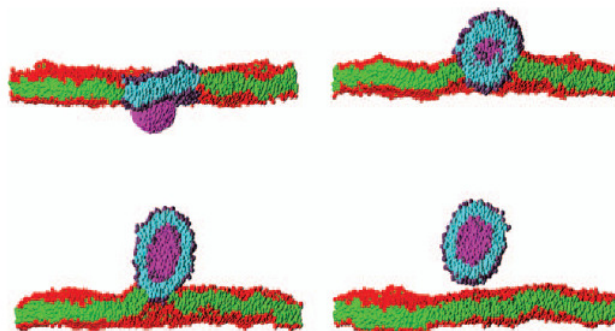


Figure 1.3: Snapshots of a cross section through a rigid nanoparticle translocating across a planar lipid bilayer membrane immersed in solvent. (*Reproduced from Shillcock [28]*).

A three-bead model [30] using non-additive, pairwise potentials between amphiphiles was proposed which resulted in self-assembling and formation of planar bilayer structure. Another example [31] considers an amphiphile as a three particle linear chain consisting of one hydrophilic head particle and two hydrophobic tail particles. A long range attractive potential between tail particles drive self-assembly.

These coarse grained simulation methods have been used to study a lot of membrane properties, both equilibrium and non-equilibrium, and is an important tool to understand interactions of NP's with the cell membrane. Rigid, spherical-cap inclusions embedded in a fluid membrane simulated with solvent-free, coarse-grained MD [32] are able to induce

membrane curvature resulting in membrane invagination which could be important to understand the endocytic pathway, a significant issue for the development of gene and drug delivery tools.

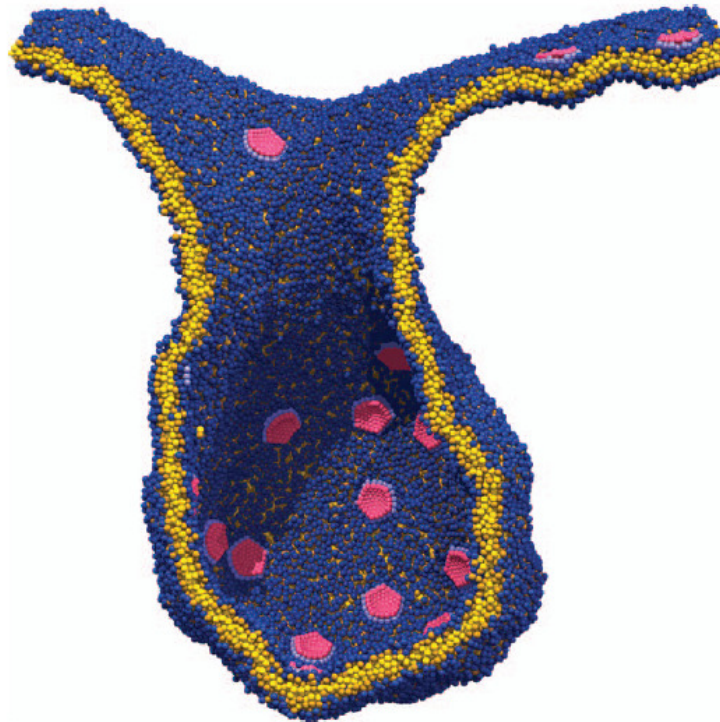


Figure 1.4: A cross section through a membrane invagination driven by the presence of rigid inclusions (*Reproduced from Deserno ([32])*)

1.5 Simulating the entire endocytic pathway

This is a non-trivial task. There have been a very few attempts to study such pathways for nanoparticle uptake. In this project, we will report about our attempt where the various processes of adsorption of nanoparticles on cell membrane, endocytosis, fate of engulfed nanoparticles inside the cells are expressed as rates and then stochastic simulations are performed.

Chapter 2

Single particle endocytosis

The endocytic process involves three important processes: the cargo needs to bind to the membrane or receptors present on the membrane which is governed by energetic and entropic balances of the membrane. Further, the membrane needs to bend in order to invaginate the particle so that the scission proteins could come and do their job. Then the particle wraps itself in a vesicle coated by the same membrane layer and is targeted to other specific organelles or vesicles. It so happens that when particles are endocytosed, then they are not often endocytosed individually but as aggregates involving two or more particles. In this chapter, however we would be considering single particle uptake and working with a minimalistic simple model. We would write down the various energy terms and try to come up with shape equations for the membrane profile. We have reproduced the results by M. Deserno. ([17]).

2.1 Various energy contributions

When a particle is adsorbed to the cell membrane, it induces deformations in the membrane which can be studied in the framework of Helfrich hamiltonian. We would assume that the membrane is fluid. The geometry of this process is depicted by the following figure : (Fig.2.1).

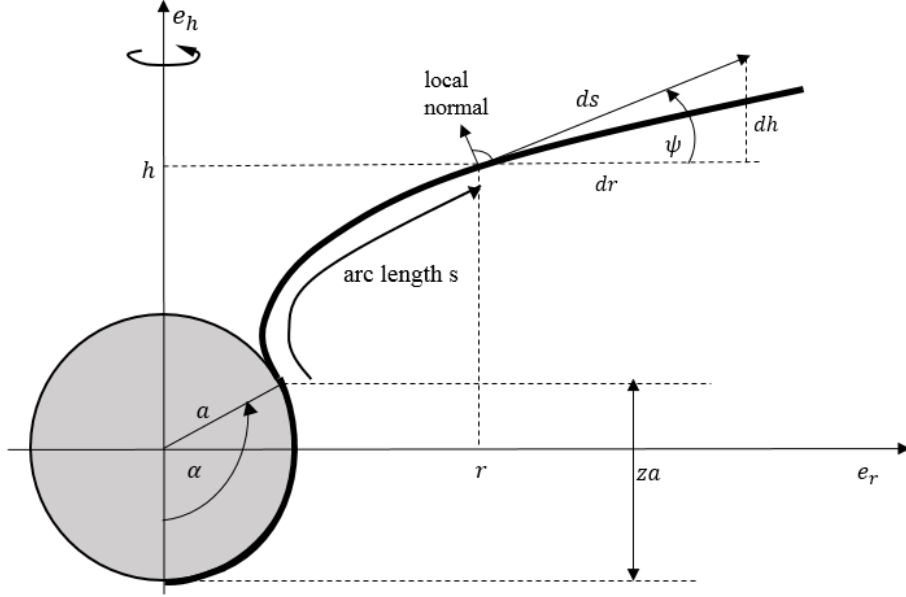


Figure 2.1: Figure representing the geometry of the wrapping process. A spherical particle of radius a wraps to the membrane with a degree of wrapping given by $z = 1 - \cos \alpha$. Cylindrical geometry is assumed.

This process can be understood as a balance of the following three energy contributions: (i) When a particle binds to the membrane, some amount of chemical energy is released, called *contact energy* per unit area w and this drives this adhesion (ii) this process is opposed by the requirement to bend the membrane and (iii) doing extra work of pulling excess membrane toward the wrapping site against a *lateral tension* σ . The bending energy per unit area is given by the standard Helfrich expression [3] that we discussed in Chapter 1.

$$e_{bend} = \frac{1}{2} \kappa (c_1 + c_2 - c_0)^2 + \bar{\kappa} c_1 c_2, \quad (2.1)$$

where c_1 and c_2 are the local principal curvatures of the membrane surface [33], c_0 is the spontaneous curvature of the membrane, and κ and $\bar{\kappa}$ are elastic moduli (with units of energy). Here, we will assume that the membrane is symmetric, i.e., spontaneous curvature is zero. ($c_0 = 0$). We would also consider that topology of the membrane is not changed upon these deformations so the second term in Eq.2.1 can be dropped. The reason for dropping the term is as follows: The product of the two principal curvatures is called the *Gaussian Curvature* ($K_G = c_1 c_2$). Its integral over a surface f can be rewritten as a line

integral of the geodesic curvature over the boundary ∂f of f (Gauss-Bonnet theorem).

$$\int_f dAK_G = 2\pi - \int_{\partial f} dsK_g, \quad (2.2)$$

for a simply connected surface. ∂f of the surface is a circle of radius R . Its geodesic curvature, K_g is $\frac{1}{R}$. Hence,

$$\int_{\partial f} dsK_g = 2\pi \quad (2.3)$$

Hence,

$$\int_f dAK_G = 0, \quad (2.4)$$

as long as no topological changes occur. Thus, we can drop the second term in Eq.2.1. The tension work is per definition given by the lateral tension σ times the excess area pulled toward the wrapping site [34].

The degree of wrapping which is a measure of how much particle has been wrapped by the membrane is given by, $z = 1 - \cos \alpha$ (Fig.2.1). The area of the particle covered by membrane is given by

$$A_{ad} = \int_0^\alpha \int_0^{2\pi} a^2 \sin \theta d\theta d\phi = 2\pi a^2 z, \quad (2.5)$$

which gives us the contact energy, $E_{ad} = -wA_{ad} = -2\pi a^2 zw$. Using Eq.2.1, the bending energy is given by $E_{bend} = \frac{1}{2}\kappa(\frac{1}{a} + \frac{1}{a})^2 A_{ad} = 4\pi z\kappa$ since the geodesic curvature of a sphere of radius R is $\frac{1}{R}$. Finally, the work done against a lateral tension σ is proportional to the excess area pulled toward the wrapping site, which is $\Delta A_{ad} = \pi a^2 z^2$, hence the tension energy, $E_{ten} = \pi a^2 z^2 \sigma$.

Now, we will introduce the following three dimensionless variables:

$$\tilde{E} = \frac{E}{\pi\kappa}, \quad (2.6)$$

$$\tilde{w} = \frac{2wa^2}{\kappa}, \quad (2.7)$$

$$\tilde{\sigma} = \frac{\sigma a^2}{\kappa} = \frac{a^2}{\lambda}, \quad (2.8)$$

where numerical factors of π and 2 have been introduced for mathematical convenience. In terms of these reduced variables the total energy of the particle-membrane complex is given by

$$\tilde{E} = -(\tilde{w} - 4)z + \tilde{\sigma}z^2 + \tilde{E}_{free}(z, \tilde{\sigma}) \quad (2.9)$$

where $\tilde{E}_{free} = E_{free}/\pi\kappa$ is the dimensionless energy of the *free* part of the membrane.

First we put $\tilde{E}_{free} = 0$ and study the behavior of \tilde{E} as a function of z . To do that we minimize \tilde{E} with respect to z . (Eq.2.9) (Fig.2.2)

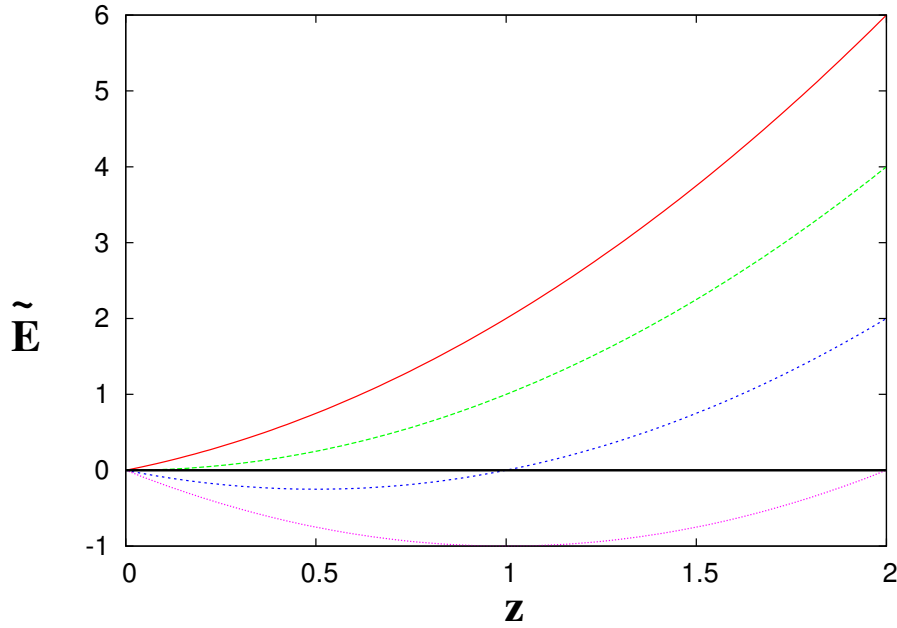


Figure 2.2: Energy \tilde{E} as a function of the penetration z for rescaled tension $\tilde{\sigma} = 1$ when $E_{free} = 0$ for different \tilde{w} . $\tilde{w} = 3$ (red), $\tilde{w} = 4$ (green), $\tilde{w} = 5$ (blue) and $\tilde{w} = 6$ (pink).

For $\tilde{w} < 4$, there is no free energy minimum and particle is not wrapped. It cannot pay the bending price. Once $\tilde{w} > 4$, the particle start to adhere by first being partially wrapped as can be seen by the development of a free energy minimum. Full envelopment occurs only if $\tilde{w} > 4 + 4\tilde{\sigma}$. In between, the degree of partial wrapping is $z = (\tilde{w} - 4)/2\tilde{\sigma}$.

2.2 Considering all the energy terms

The part of the membrane which is close to the line of contact is very curved and therefore we cannot neglect \tilde{E}_{free} . In this section, we obtain an expression for this part of the membrane which plays an important role in the overall free energy.

2.2.1 Full energy term and shape equations

The energy of the free membrane is the surface integral over the local bending and tension contributions and is thus a functional of the shape. Using the geometry from Fig.2.1, the two principal curvatures are found to be $\frac{\sin\psi}{r}$ and $\dot{\psi}$, where the dot indicates a derivative with respect to the arclength s . These two principal curvatures can be derived from the expressions that $c_1 = \partial n_r / \partial r$ and $c_2 = \partial n_h / \partial h$. Using Fig.2.1, we can identify them. The energy functional can then be written as [8] [10] [11]

$$\tilde{E}_{free} = \int_0^\infty ds L(\psi, \dot{\psi}, r, \dot{r}, \dot{h}, \lambda_r, \lambda_h), \quad (2.10)$$

where the Lagrangian L is defined by,

$$L = r \left[\left(\dot{\psi} + \frac{\sin \psi}{r} \right)^2 + \frac{2\tilde{\sigma}}{a^2} (1 - \cos \psi) \right] + \lambda_r (\dot{r} - \cos \psi) + \lambda_h (\dot{h} - \sin \psi) \quad (2.11)$$

The expression in square brackets contains the bending and tension contributions. The first term in it is the Helfrich bending energy with the values of both principal curvatures. The second term is the tension term with the excess membrane deformed by an angle ψ . The last two additional terms are introduced due to the parametrization constraints $\dot{r} = \cos \psi$ and $\dot{h} = \sin \psi$ where $\lambda_r(s)$ and $\lambda_h(s)$ are Lagrange parameters.

We are interested in evaluating Hamilton's equations of motion. So, we switch to a Hamiltonian description. The conjugate momentum is defined as $p_{q_i} = \frac{\partial L}{\partial \dot{q}_i}$ where q_i is a generalized coordinate and p_{q_i} is the corresponding conjugate momentum. Hence, the conjugate momenta for the energy functional are :

$$p_\psi = \frac{\partial L}{\partial \dot{\psi}} = 2r\dot{\psi} + \frac{\sin \psi}{r}, \quad (2.12)$$

$$p_r = \frac{\partial L}{\partial \dot{r}} = \lambda_r, \quad (2.13)$$

and

$$p_h = \frac{\partial L}{\partial \dot{h}} = \lambda_h, \quad (2.14)$$

Now, since $H = \sum p\dot{q}_i - L$, hence

$$H = \dot{\psi}p_\psi + \dot{r}p_r + \dot{h}p_h - L = \frac{(p_\psi)^2}{4r} - \frac{p_\psi \sin \psi}{r} - \frac{2\tilde{\sigma}r}{a^2}(1 - \cos \psi) + p_r \cos \psi + p_h \sin \psi \quad (2.15)$$

Using the above equations, the Hamilton's equations for the membrane are :

$$\dot{\psi} = \frac{p_\psi}{2r} - \frac{\sin \psi}{r}, \quad (2.16)$$

$$\dot{r} = \cos \psi, \quad (2.17)$$

$$\dot{h} = \sin \psi, \quad (2.18)$$

$$\dot{p}_\psi = \left(\frac{p_\psi}{r} - p_h\right) \cos \psi + \left(\frac{2\tilde{\sigma}r}{a^2} + p_r\right) \sin \psi, \quad (2.19)$$

$$\dot{p}_r = \frac{p_\psi}{r} \left(\frac{p_\psi}{4r} - \frac{\sin \psi}{r}\right) + \frac{2\tilde{\sigma}}{a^2}(1 - \cos \psi), \quad (2.20)$$

and

$$\dot{p}_h = 0. \quad (2.21)$$

2.2.2 Necessary boundary conditions

Initially the membrane is flat and then it wraps around the spherical particle. Therefore, at the contact boundary, $s = 0$, we will have (Fig.2.1):

$$r(0) = a \sin \alpha, \quad (2.22)$$

$$h(0) = -a \cos \alpha, \quad (2.23)$$

and

$$\psi(0) = \alpha. \quad (2.24)$$

Since the membrane becomes flat at large distances from the wrapping region, hence we must have,

$$\lim_{s \rightarrow \infty} \psi(s) = 0 \quad (2.25)$$

$$\lim_{s \rightarrow \infty} \dot{\psi}(s) = 0 \quad (2.26)$$

We numerically solve the set of equations with appropriate boundary conditions using the shooting method. The total free energy shows that for $\tilde{w} < 4$, there is no wrapping. For $\tilde{w} = 4$, we get partial wrapping. For $\tilde{w} > 4$, the energy of fully wrapped state is lowered. (Fig.2.3)

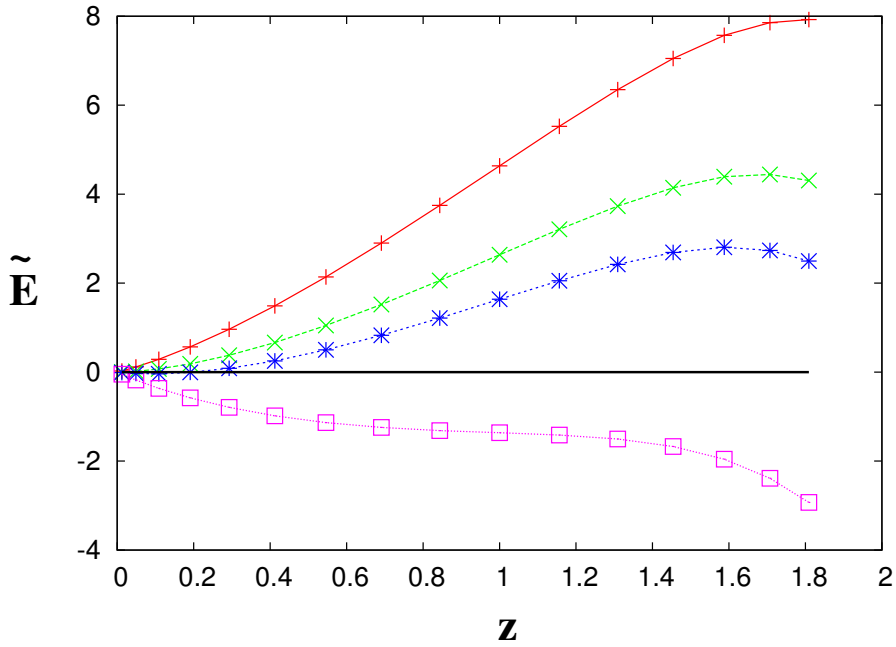


Figure 2.3: Energy \tilde{E} as a function of the penetration z for rescaled tension $\tilde{\sigma} = 1$ when $E_{\text{free}} \neq 0$ for different \tilde{w} . $\tilde{w} = 3$ (red), $\tilde{w} = 4$ (green), $\tilde{w} = 5$ (blue) and $\tilde{w} = 6$ (pink).

Also, if $\psi(s)$ vanishes rapidly, we can say that all contributions beyond some large distance S in arclength will be negligible. So, we can use this condition and say that we choose an upper arclength S and impose the zero angle condition there. Hence, S and $\psi(S)$ do not vary during functional minimization, but the parameters $r(S)$ and $h(S)$ are still free. So we

fix them by imposing additional boundary conditions : [11] [35]

$$0 = \left. \frac{\partial L}{\partial \dot{r}} \right|_{s=S} = p_r(S) \quad (2.27)$$

and

$$0 = \left. \frac{\partial L}{\partial \dot{h}} \right|_{s=S} = p_h(S) \quad (2.28)$$

Now, according to the Hamilton equation, Eq.2.21, we can say that p_h is an integral of *motion* and hence the boundary condition Eq.2.28 determines its value to be zero. Hence, we do not have to worry about p_h anymore. Now we need to take care of the condition on p_r . Now, if the angle ψ converges to zero, the expression for the Hamiltonian converges toward p_r (from Eq.2.15). Thus, the requirement of a flat profile implies $H = H(S) \rightarrow p_r(S) = 0$, or we can say that, if the membrane is to become flat, the Hamiltonian must be zero. Using Eqs. 2.2.1 and 2.15, we can find out a condition for p_r at the *contact* boundary:

$$ap_r(0) = \frac{\sqrt{z(2-z)}}{1-z} (1 + 2\tilde{\sigma}z - [a\dot{\psi}(0)]^2) \quad (2.29)$$

The only remaining variable for which the contact value is not yet known is p_ψ , or alternatively $\dot{\psi}$. It is the condition of asymptotic flatness that will determine $\dot{\psi}_0$.

Therefore, in this chapter we have looked at the various energetics involved when a membrane wraps around a single spherical particle. Although, the shape and size of the nanoparticle will matter, we can see that adhesion and bending are key players in this process. How particle size can matter can also be understood from the above analysis where we can see that below $\tilde{w} < 4$, there will be no wrapping. Recall that $\tilde{w} = \frac{2wa^2}{\kappa}$, therefore $\tilde{w} < 4$ implies $a < \sqrt{\frac{2\kappa}{w}}$ which gives a length scale for the particle size. So particles below $\sqrt{\frac{2\kappa}{w}}$ will not be wrapped.

Chapter 3

Multiscale modeling of nanoparticle transport across the cell membrane

In the last chapter, we considered single particle endocytosis, wrote down various energy terms for the process and came up with the shape equations for the membrane profile. In this chapter, we will study the dynamics of several such nanoparticles as they are internalized both analytically and using computer simulations. For our simulations, we use the package called Smoldyn, which considers the particles as point particles and performs overdamped Langevin dynamics.

Endocytosis is a highly complex mechanism which the cell uses not only to take up nutrients but also in cell-cell communication. After the endocytosis process is complete, the internalized cargo then undergoes a series of dynamic processes like fission, fusion and degradation, which define the endocytic pathway. We try to understand the dynamics of nanoparticle transport across the cell membrane and its subsequent dynamics inside the cell. In this work, we shall additionally assume that nanoparticles contain cargo molecules which have to be transported inside the cell. This has very important implications in the context of drug delivery. For example, experimentally people use polymersomes which are diblock copolymer vesicles to transport drug molecules inside the cell. These polymersomes have the drug molecules inside them and their sizes are of the order of a few tens of nanometers. So, they can be thought as good examples of our model system. We first do a multiscale modeling of transport across the cell membrane. We specifically study nanoparticle mediated cargo transport and the effect of the release of the cargo from the nanoparticles both inside and outside the cell. We show quantitatively how diffusion and the rates of adsorption/desorption from the cell membrane play an important role in cargo

transport. We draw phase diagrams which indicate regions for optimal transport. We also incorporate nanoparticle size in our simulations and extract endocytosis rates which are predicted to be dependent on their size.

3.1 Endocytic Transport

We first consider a very simple system where nanoparticles are getting adsorbed on the cell surface and then they are endocytosed. From now onwards we ignore the complex endocytic process of adsorption, wrapping and pinching off and consider only rates of the various processes. Therefore, nanoparticles are adsorbed to the surface with a rate k_a ; they can be desorbed at the rate k_d ; internalization happens with a rate k_e and particles can be thrown back outside the cell with rate k_{rec} . The last process is called *exocytosis*. The set of equations is as follows :

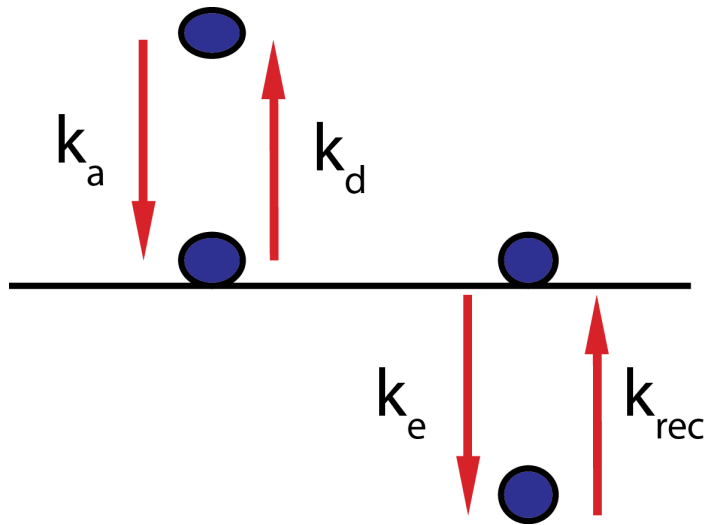


Figure 3.1: Model of the system.

Equations governing uptake:

$$\frac{dc_{ex}}{dt} = -k_a c_{ex} + k_d c_m \quad (3.1)$$

$$\frac{dc_m}{dt} = k_a c_{ex} - (k_d + k_e) c_m + k_{rec} c_i \quad (3.2)$$

$$\frac{dc_i}{dt} = k_e c_m - k_{rec} c_i \quad (3.3)$$

where c_{ex} is the concentration of particles outside the cell; c_m is the concentration of particles on the surface and c_i is the concentration of internalized particles.

In these equations, all rates are in units of $time^{-1}$. This set of coupled differential equations can be solved by Laplace transform. The resulting internalized particle concentration is given by

$$c_i(t) = \frac{k_a k_e c_{ex}^0}{\lambda_+ \lambda_- (\lambda_+ - \lambda_-)} [(\lambda_+ - \lambda_-) + \lambda_- e^{-\lambda_+ t} - \lambda_+ e^{-\lambda_- t}] \quad (3.4)$$

where

$$\lambda_{\pm} = \frac{(k_d + k_e + k_a + k_{rec}) \pm \sqrt{(k_d + k_e + k_a + k_{rec})^2 - 4(k_d k_{rec} + k_a k_e + k_a k_{rec})}}{2} \quad (3.5)$$

and c_{ex}^0 is the extracellular concentration of particles at time $t = 0$. The behavior at $t \rightarrow \infty$ is simple and we get

$$\frac{c_i(t \rightarrow \infty)}{c_{ex}^0} = \frac{k_a k_e}{k_d k_{rec} + k_a k_e + k_a k_{rec}} \quad (3.6)$$

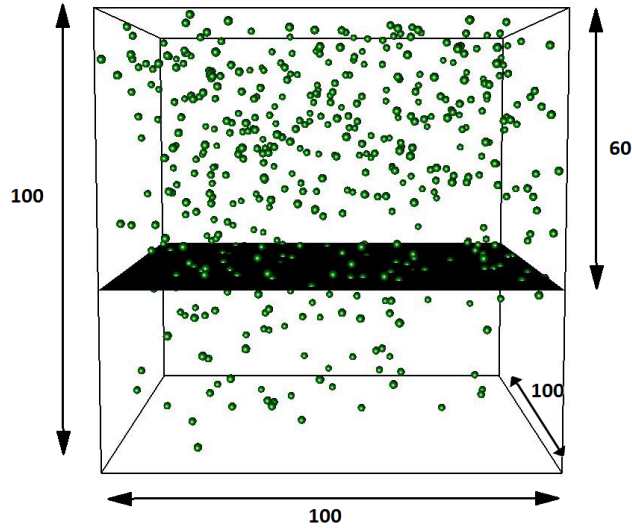


Figure 3.2: Snapshot of the system.

To get the steady state features of this system in simulation, we take a cubic box separated

by a surface. The upper half of the box is the extracellular region while the lower half is the cell. The flat surface separating the two is the cell membrane. As we have mentioned before, we discard all structures of the membrane and only consider rates of the various processes. The simulation starts with a concentration of nanoparticles (point particles in Smoldyn), in the extracellular region and then there are rates for adsorption, desorption, endocytosis and exocytosis. In the simulation, the rates are chosen as follows: $k_d = 1.0$ and $k_e = 1.0$. We do not need to change these as they are in units of $1/time$. $k_a = 1.0$ and in Smoldyn, this rate is in the units of $length/time$ in the code. Therefore to change it into $1/time$ units we multiply by the concentration ($1/length^3$) and the surface area ($length^2$). The available volume for the particles when they are released is $((100 * 100 * 100) - (40 * 100 * 100))$ since the inner cell where the particles are internalized has the volume of $40 * 100 * 100$. Therefore the adsorption rate $k_a = 1.0 * 100 * 100 / ((100 * 100 * 100) - (40 * 100 * 100))$ in units of $1/time$. The recycling rate, $k_{rec} = 1.0$ in the code. This rate is again in units of $length/time$. So to change to $1/time$ units we multiply by inverse volume which in this case is $40 * 100 * 100$ and the surface area which is the same as before $100 * 100$. Therefore $k_{rec} = 0.1 * 100 * 100 / (40 * 100 * 100)$.

We plot the normalized concentration of internalized particles as a function of time for different recycling rates. As k_{rec} is decreased, lesser number of particles which enter the cell are thrown out. Thus, the saturation levels of normalized uptake in the steady state are higher. We match our steady state values with those obtained from our deterministic equation. They are expected to match and that is observed in the figure. In Fig.3.3, the solid line is the theoretical behavior at $t \rightarrow \infty$.

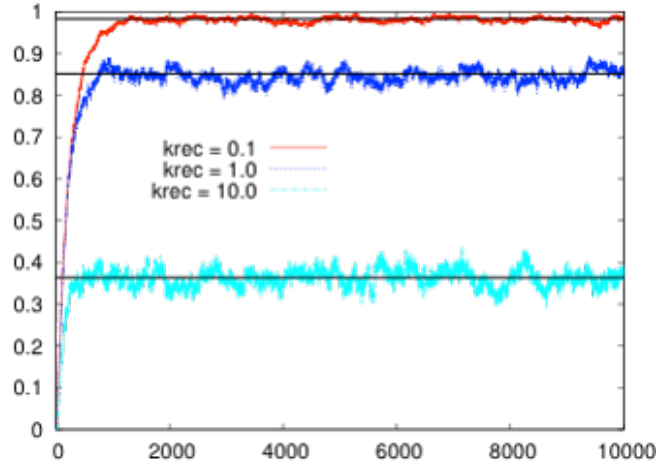


Figure 3.3: $\frac{c_i(t \rightarrow \infty)}{c_{e,x}^0}$ as a function of time.

3.2 Modeling transport of nanoparticles carrying cargo

We study carrier mediated cargo transport and the effect of the release of the cargo from the nanoparticles (herewith called nano-carriers) both inside and outside the cell. Our model environment comprises a single cell and a limited volume of immediately adjacent nanoparticles as considered in the previous section. We assume the presence of cargo carrier nanoparticles in the outer side and follow the transport of these carriers and the cargo that they release in the course of their movement from the outside to the inside via transcytosis across the cell.

The nano-carrier diffuses in the region outside the cell and may release the cargo molecules either inside or outside the cell volume. We assume that once the cargo molecules reach the bottom surface of the cell to the other side, they are absorbed. This marks a successful transcytosis event. For the sake of simplicity, we assume that only cargo molecules (and not the nano-carriers) are absorbed to the other side.

We start with N nano-carriers in the volume outside the cell. They diffuse with a diffusion coefficient D_p . A nano carrier can break up to release the cargo. Since in Smoldyn, the particles are point particles, this is incorporated as a reaction as follows: $1 \text{ Carrier} \rightarrow n \text{ Cargo}$. This process of degradation has a rate associated with it. This rate can be varied depending on whether the cargo is released outside or inside the cell. Therefore, we consider

two possible scenarios:

Cargo released outside The cargo is released outside the cell cytoplasm with a rate k_{oc} . Once released the cargo molecules diffuse with diffusion coefficient given by D_d . During diffusion, they come in contact with the cell membrane and bind/unbind to the cell surface with adsorption/desorption rates k_{ad} , k_{dd} respectively. The adsorbed cargo molecules are endocytosed with a rate k_{end} . Once inside the cell volume, they diffuse and are adsorbed on the surface of the cell on the other side with a rate k_t . In this state we say that the cargo molecule is transported from one side to the other side. To incorporate efflux mechanisms, the freely diffusing cargo molecules inside the cell cytoplasm could be exocytosed to the source side with a rate k_{exd} .

Cargo released inside The cargo is released inside the cell cytoplasm with a rate k_{ic} . The nano-carriers carrying the cargo molecules are adsorbed/desorbed at the cell surface with rates k_{pd} , k_{dd} respectively and are subsequently endocytosed with a rate k_{enp} . Once in, they release the cargo inside the cytoplasm. The cargo molecules diffuse and are adsorbed to the other side with the rate k_t . Note that the nano-carriers may be thrown out of the cytoplasm with rate k_{exp} .

Hence, we have the following rates:

- k_{oc} : Rate of cargo release outside cytoplasm.
- k_{ic} : Rate of cargo release inside cytoplasm.
- k_{ap} , k_{dp} : Rate of attachment/detachment of nanoparticle (containing cargo) to the membrane surface.
- k_{ad} , k_{dd} : Rate of attachment/detachment of cargo to the membrane surface.
- k_{enp} , k_{exp} : Rate of endo/exocytosis of nanoparticle.
- k_{end} , k_{exd} : Rate of endo/exocytosis of cargo.
- k_t : Rate of transcytosis.

For the situation where the nanoparticle releases the cargo outside the cell, we plot the uptake of cargo as a function of the time for different rates of endocytosis. The uptake increases for increasing rates of endocytosis as expected. The exocytosis rate is kept fixed.

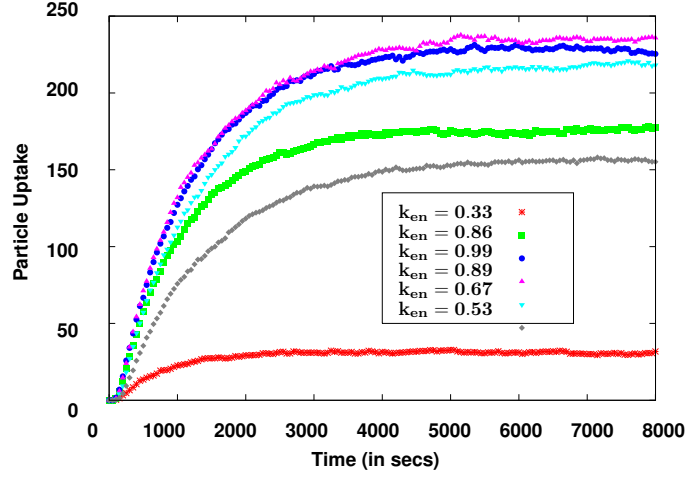


Figure 3.4: Normalized particle uptake versus time for different endocytosis rates of the cargo.

We first make some simplifying assumptions. Assume that there is no exocytosis of cargo or nanoparticle i.e. $k_{exp} = 0 = k_{exd}$ and that there is no detachment of cargo or nanoparticle from the membrane surface once it is bound, i.e. $k_{dp} = 0 = k_{dd}$. Also note that if the cargo is released outside the cytoplasm, then $k_{ap} = 0$. Finally assume that the attachment rates of both cargo and nanoparticle are the same : $k_{ap} = k_{ad} = k$. Expressing all rates in units of k , we have the following rates to vary : $k_{oc}, k_{ic}, k_{enp}, k_{end}$. Also, $D_d = 10D_p$.

We next make a comparative study for cargo released inside and outside the cell. For different rates of k_{ic}/k_{oc} , we find that the time for complete transcytosis of cargo would be vastly different depending on the different rates of endocytosis. Note that in this set of studies, the exocytosis rates are set to zero. We find that in terms of the time it takes for all cargo molecules to be endocytosed, effective uptake takes place when cargo is released inside the cell rather than both inside and outside. This is significant in the context that it has meritorious applications in drug-delivery mechanism. One can adjust the drug release process and endocytosis rates while designing the methods for drug targeting and at that point it becomes important if one already knows the optimal drug release route and rates.

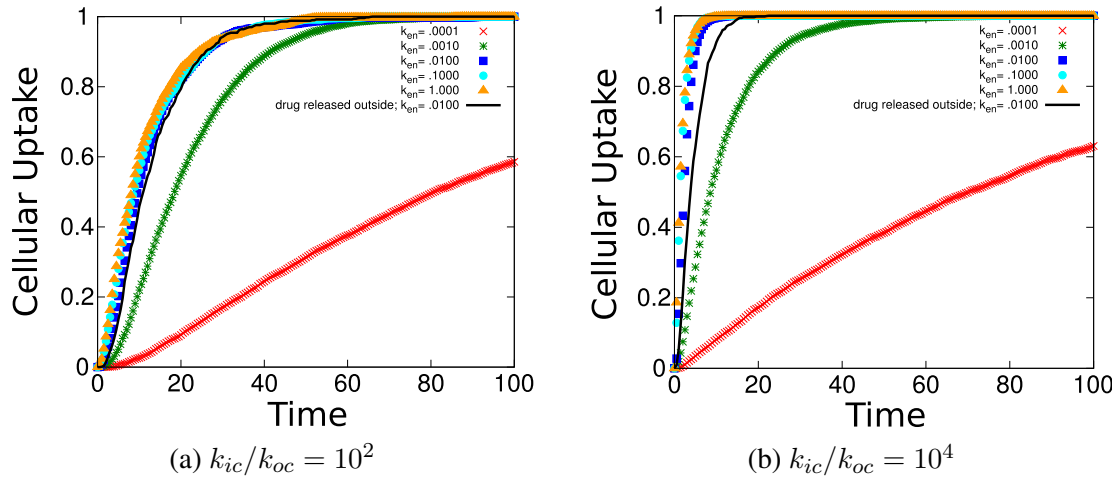


Figure 3.5: Normalized cellular uptake for different endocytosis rates for different ratios of k_{ic}/k_{oc} .

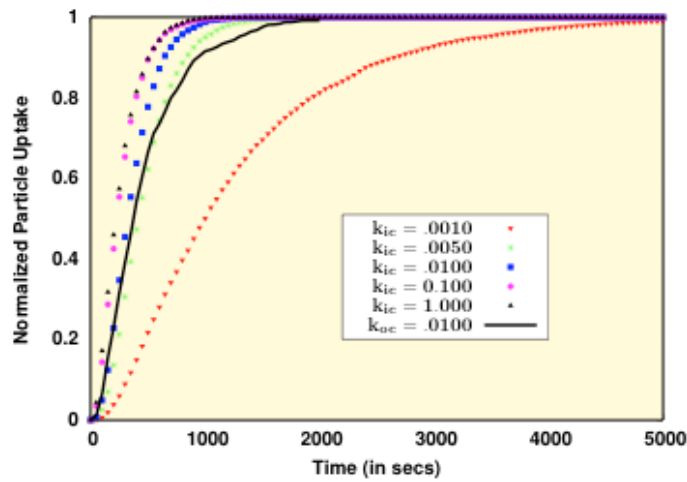


Figure 3.6: Normalized particle uptake for different k_{ic}/k_{oc} rates.

The phase diagram below indicates regions for optimal uptake of cargo depending on the rates of diffusion coefficients of nanoparticles and cargo and on the rates of k_{oc} and k_{ic} (Fig.3.7).

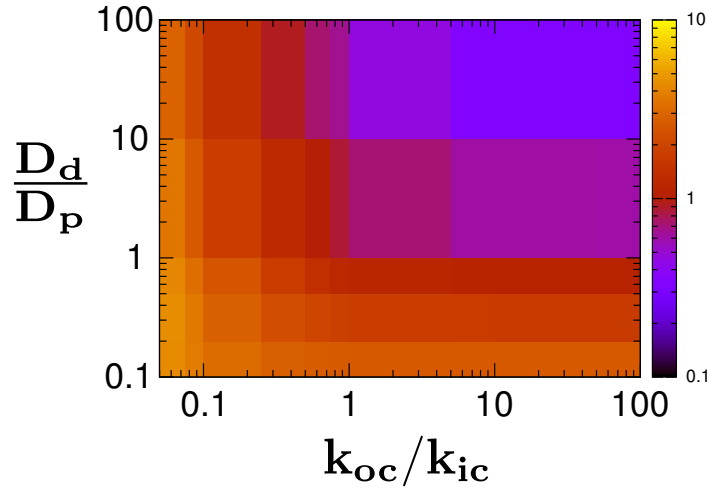


Figure 3.7: Phase diagram indicating regions for optimal transport. Color bar is the time axis.

3.2.1 Size dependent cellular uptake

As we have seen in the last chapter, theoretical studies predict a threshold radius below which there can be no cellular uptake. Also, the distribution of uptake is asymmetric. To incorporate size dependence in our simulation system is tricky. As pointed out earlier, Smoldyn considers point particles. The way we incorporate this is to take the theoretical plot of the normalized uptake as a function of nanoparticle radius and use the same plot for the endocytosis rates of nanoparticles [36]. In other words, we choose a distribution of endocytosis rates which follow the theoretical plot. Obviously we have to distinguish the particles. This is done by choosing different diffusion coefficients which goes as the inverse of the radius of the nanoparticles obtained from the theoretical plot. Therefore we start with a set of nanoparticles each of which has a specific endocytosis rate and a specific diffusion coefficient. If we now do simulation of such a system and obtain the nanoparticle uptake as a function of time, then the steady state normalized uptake values for each set of nanoparticles should have the same distribution as a function of nanoparticle radius as predicted theoretically.

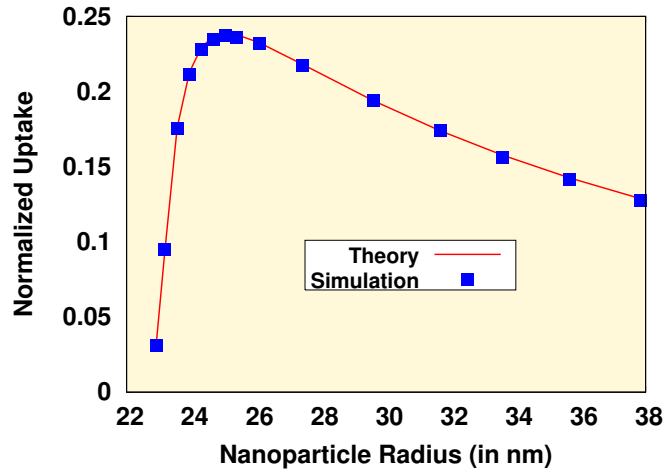


Figure 3.8: Size dependent cellular uptake of non-interacting NP's.

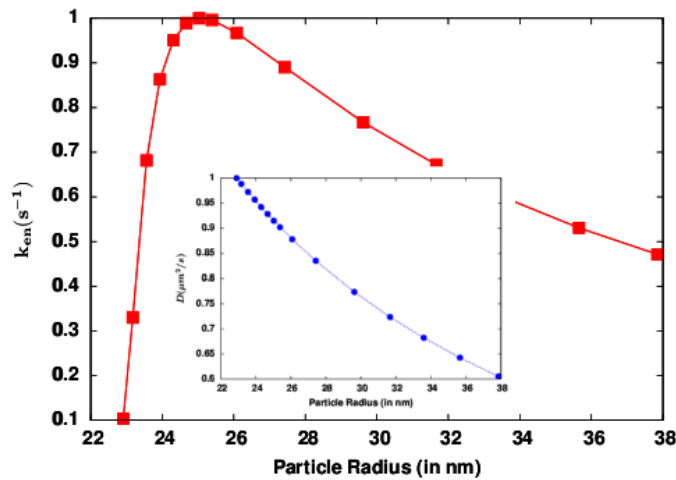


Figure 3.9: Size dependent variation of endocytosis rate.

3.3 Conclusions

Endocytosis is a very important process and it's necessary that one should know the mechanics and dynamics given the fact that it has far reaching applications in drug delivery. In this work, we have tried to investigate the nanoparticle uptake by a cell taking into account parameters like nanoparticle size, diffusion coefficients, attachment/detachment and

endocytosis rates. We have tried to identify the optimal parameters for efficient particle uptake.

Bibliography

- [1] B. Alberts, A. Johnson, J. Lewis, M. Raff, K. Roberts, and P. Walter, *Molecular Biology of the Cell*. Garland Publishing, New York, NY, fourth edition, (2002).
- [2] Canton I. and Battaglia G., *Chem Soc Rev*. 2012 Apr 7;41(7):2718-39. doi: 10.1039/c2cs15309b. Epub 2012 Mar 5.
- [3] W. Helfrich, *Z. Naturforsch.* **28c**, 693 (1973).
- [4] P. B. Canham, *J. theor. Biol.* **26**, 61 (1970).
- [5] R. Lipowsky, *Nature* **349**, 475 (1991).
- [6] R. Lipowsky, *Biophys. J.* **64**, 1133 (1993).
- [7] R. Lipowsky and E. Sackmann, Structure and dynamics of membranes, Vol. 1 of Handbook of biological physics (Elsevier, Amsterdam, 1995)
- [8] U. Seifert, *Adv. Phys.* **46**, 13 (1997).
- [9] F. Julicher and R. Lipowsky, *Phys. Rev. E* **53**, 2670 (1996).
- [10] U. Seifert, K. Berndl, and R. Lipowsky, *Phys. Rev. A* **44**, 1182 (1991).
- [11] F. Julicher and U. Seifert, *Phys. Rev. E* **49**, 4728 (1994).
- [12] L. Miao, B. Fourcade, M. Rao, M. Wortis, and R. K. P. Zia, *Phys. Rev. A* **43**, 6843 (1991).
- [13] S. Svetina and B. Zeks, *Eur. Biophys. J.* **17**, 101 (1989).
- [14] U. Seifert and R. Lipowsky, *Phys. Rev. A* **42**, 4768 (1990).
- [15] U. Seifert, *Phys. Rev. Lett.* **74**, 5060 (1995).
- [16] M. Deserno and T. Bickel *Europhys. Lett.* **62**, 767 (2003).

- [17] M. Deserno, Phys. Rev. E **69**, 031903, (2004)
- [18] T. R. Powers, G. Huber, and R. E. Goldstein, Phys. Rev. E **65**, 041901 (2002).
- [19] I. Derenyi, F. Julicher, and J. Prost. Phys. Rev. Lett. **88**, 238101 (2002).
- [20] A.-S. Smith, E. Sackmann, and U. Seifert, Europhys. Lett. **64**, 281 (2003).
- [21] A.-S. Smith, E. Sackmann, and U. Seifert, Phys. Rev. Lett. **92** 208101 (2004).
- [22] G. Koster, A. Cacciuto, I. Derenyi, D. Frenkel, and M. Dogterom. Phys. Rev. Lett. **94** 068101 (2005).
- [23] J. Liu, Y.D. Sun, D.G. Drubin and G.F. Oster Plos Biology **7**, e1000204 (2009).
- [24] M. Muller, K. Katsov and M. Schick Phys. Rep. **434** 113 (2006).
- [25] M. Venturoli, M. M. Sperotto, M. Kanenburg and B. Smit Phys. Rep. **437**, 1 (2006).
- [26] J. C. Shillcock and R. Lipowsky Nat. Mater. **4**, 225 (2005).
- [27] J. C. Shillcock and R. Lipowsky J. Phys.: Condens. Matter **18**, S1191 (2006).
- [28] J. C. Shillcock HPSP J. **2**, 1 (2008).
- [29] M. P. Allen and D. J. Tildesley Computer Simulation of Liquids, Oxford Science Publications, OUP, Oxford, UK (1987).
- [30] O. Farago J. Chem. Phys. **119**, 596 (2003).
- [31] I. R. Cooke, K. Kremer and M. Deserno, Phys. Rev. E **72**, 011506 (2005).
- [32] B. J. Reynwar, G. Illya, V. A. Harmandaris, M. M. Mller, K. Kremer, and M. Deserno Nature (London) **447**, 461 (2007).
- [33] E. Kreyszig, *Differential Geometry (Dover, New York, 1991)*.
- [34] F. David and S. Leibler, *J. Phys. II* **1**, 959 (1991).
- [35] R. Courant and D. Hilbert, *Methods of Mathematical Physics (Interscience, New York, 1953), Vol. 1*.
- [36] Abhishek Chaudhuri, Giuseppe Battaglia and Ramin Golestanian, *The effect of interactions on the cellular uptake of nanoparticles, 2011 Phys. Biol.* **8** 046002.